Eur. Phys. J. D **13**, 271–278 (2001)

THE EUROPEAN PHYSICAL JOURNAL D

EDP Sciences

Atomic diffraction by a laser standing wave: Analysis using Bloch states

C. Champenois, M. Büchner, R. Delhuille, R. Mathevet, C. Robilliard, C. Rizzo, and J. Vigué[a]

Laboratoire Collisions Agrégats Réactivité, IRSAMC, Université Paul Sabatier[b], 118 route de Narbonne, 31062 Toulouse Cedex, France

Received 10 July 2000 and Received in final form 15 September 2000

Abstract. Atomic diffraction by a laser stationary wave is commonly used to build mirrors and beam splitters for atomic interferometers. Many aspects of this diffraction process are well understood but it is difficult to get an unified view of this process because it is commonly described in several approximate ways. We want to show here that a description inspired by optics and using the exact Bloch description of the atomic wave inside the laser standing wave is a tutorial way of describing the various regimes by a single formalism. In order to get simple analytic expressions of the diffraction amplitudes, we consider a standing wave intensity with a flat transverse profile. The resulting general expression of the diffraction intensities is then compared to available analytical formulae in the Raman-Nath limit and in the Bragg regime. We think that this formalism can be fruitfully extended to study many important questions.

PACS. 39.20.+q Atom interferometry techniques – 42.50.Ct Quantum description of interaction of light and matter; related experiments – 03.75.-b Matter waves

1 Introduction

We discuss here the diffraction of an atomic wave by a laser standing wave. We assume that the laser detuning is sufficient so that real population of the resonantly excited state is negligible so that spontaneous emission can be neglected. The only effect of the laser is then to create a potential proportional to the laser power density. Atomic diffraction results from the periodic character of this potential and the present results can be easily generalized to various types of periodic potentials.

Many works have already been devoted to this diffraction process. We will quote the observation of the Kapitza-Dirac diffraction of atoms by Pritchard and coworkers [1–5], the observation of Bragg diffraction by the same group [6] further studied by Siu Au Lee and coworkers [7,8] and by Zeilinger and coworkers [9–13]. Many papers studying theoretically this process should also be quoted and by lack of space, we will quote only two early works [14,15] and a recent review [16].

When compared to previous works, the original character of the present treatment is the use of Bloch states to describe the atomic motion inside the laser standing wave. The application of Bloch states to atomic motion has been initially discussed by Castin and Dalibard [17]. The associated quantum dynamics was first observed experimentally in 1996, by Salomon and co-workers [18] and by Raizen and coworkers [19]. The present formalism appears somewhat implicitly in two papers published in 1999, in a theoretical paper by Horne, Jex and Zeilinger [20] which discusses Bragg scattering as solutions of the Mathieu equation and in the discussion of an experimental paper by Keller *et al.* [21]. Here, we introduce explicitly the Bloch atomic states: this point of view is very tutorial and it simplifies considerably the discussion. In this way, our discussion goes further than these two recent papers [20,21].

2 The problem

The problem treated here is the simplest case of atomic diffraction by a laser standing wave. The quasi-resonant laser waves propagate along the $\pm\mathbf{x}$-direction and we assume that the laser beams are not limited in the $\mathbf{y}$-direction. The atom is assumed to be in its ground state. If the laser detuning is sufficient, no real excitation will occur and in the dressed-atom picture [22], one shows that the only effect of the laser standing wave is to create a light shift potential $V(x,z)$:

$$V(x,z) = V_0(z)\cos^2(k_{\mathrm{L}}x) = \frac{V_0(z)}{4}\left[2+\exp(+\mathrm{i}k_{\mathrm{g}}x)+\exp(-\mathrm{i}k_{\mathrm{g}}x)\right] \quad (1)$$

where the grating wavevector k_{g} is related to the laser wavevector k_{L} by $k_{\mathrm{g}} = 2k_{\mathrm{L}}$. As the potential has no dependence on y, the motion along y is free. It will not

[a] e-mail: jacques@yosemite.ups-tlse.fr
[b] UMR 5589 du CNRS

be discussed anymore and its contribution to the kinetic energy will also be forgotten. We have to solve the following Schrödinger equation in its time independent form:

$$-\frac{\hbar^2}{2m}\left(\frac{\partial^2\Psi}{\partial x^2}+\frac{\partial^2\Psi}{\partial z^2}\right)+V(x,z)\Psi=\frac{\hbar^2k_1^2}{2m}\Psi \qquad (2)$$

where k_1 is the atomic wavevector in free space. Throughout the present paper, we will assume that $V_0(z)$ is everywhere considerably smaller than the total energy E given by the initial kinetic energy, $E=\hbar^2k_1^2/2m$. This assumption is interesting as it simplifies the calculations in several places but it is not fundamental and it can be easily relaxed. Using this approximation, one can relate the time-independent picture used here to an equivalent time-dependent picture (see Appendix A). Then, neglecting in the potential the term which does not depend on x, equation (2) takes the form:

$$\frac{\partial^2\Psi}{\partial x^2}+\frac{\partial^2\Psi}{\partial z^2}+k_1^2\left(1-\frac{V_0(z)\cos(k_{\rm g}x)}{2E}\right)\Psi=0. \qquad (3)$$

In this paper, except in Section 7, we assume that the laser has a flat intensity profile so that the potential amplitude $V_0(z)$ is nonzero and constant (noted V_0) between $z=0$ and $z=D$. This is a rather rough approximation of real experiments, but this assumption is necessary to make the problem as simple as possible. The general case requires numerical integration, if we except some particular cases as the one discussed in Section 7.

Equation (3) is completely similar to the wave equation describing diffraction of light by sound waves [23,24] which is recalled in Appendix B. This is a well known result as it is possible to define an index of refraction n related to the potential $V(x,z)$ by:

$$n^2=1-\frac{V(x,z)}{E}\cdot \qquad (4)$$

Moreover, the calculation presented here is similar in its content to the one presented in an early work of Wagner [23].

The principle of our treatment is to write the general solution for the atomic wave in three regions: region 1 which is the vacuum for $z\leq 0$, region 2 which is the grating for $0\leq z\leq D$, and region 3 which is the vacuum for $z\geq D$ (see Fig. 1). Then, as in optics when establishing Fresnel laws, we apply the continuity equations for the atomic wave in the planes $z=0$ and $z=D$.

3 Atomic Bloch states inside the laser standing waves

The motion of an atom inside the grating is free along the z-direction and is described by plane waves. The motion along the x-direction is described by Bloch states introduced in the domain of atom optics by Castin and Dalibard [17]. We first recall briefly some general results, which can be found in any solid state physics book. In the presence of a periodic potential, the eigenstates $\Psi(x)$ of the Hamiltonian can be written as

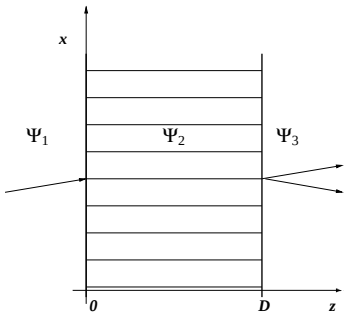

Fig. 1. In this figure, we define three different regions of space as discussed in Section 4. For $z<0$ and $z>D$, the atomic wave Ψ_1 or Ψ_3 propagates in free space, while in the range $0<z<D$, the atomic wave Ψ_2 interacts with the potential $V(x,z)$ which plays the role of a thick grating.

$$\Psi_{k,p}(x)=\exp(\mathrm{i}kx)\,u_{k,p}(x) \qquad (5)$$

where $u_{k,p}(x)$ are periodic functions of x, with a period $a=2\pi/k_{\rm g}$ equal to the grating period. In other words, the Fourier transform of a Bloch state contains only components whose wavevector along $\mathbf{x}$ are $pk_{\rm g}+k$ where p is an integer. The quasi-momentum k can always be chosen inside the first Brillouin zone (*i.e.* $-k_{\rm g}/2<k\leq k_{\rm g}/2$) and we assume that it is the case. If the potential vanishes, the eigenstates remain plane waves with a well defined wavevector k_x and we may define the index p by:

$$k_x=pk_{\rm g}+k \qquad (6)$$

and we may use this integer to label the various energy bands. The energy as a function of k is the well-known folded parabola (see Fig. 2):

$$\varepsilon_0(k,p)=\hbar^2(pk_{\rm g}+k)^2/2m. \qquad (7)$$

Equation (7) introduces the natural energy scale of the problem, the atom recoil energy given by $\hbar\omega_{\rm rec}=\hbar^2k_{\rm L}^2/2m=\hbar^2k_{\rm g}^2/8m$. It is convenient to measure the potential in this energy unit, by introducing a dimensionless parameter q defined by [21]:

$$q=V_0/(4\hbar\omega_{\rm rec}). \qquad (8)$$

In the presence of the potential given by equation (1), the Bloch eigenstates are mixtures of plane waves with the same k value and different values of the index p and their modified energies are noted $\varepsilon(k,p)$. More precisely, the potential terms proportional to $\exp(\pm\mathrm{i}k_{\rm g}x)$ couple states with p values differing by ±1. When q is small, this structure of the coupling terms makes that a perturbative viewpoint is very useful. The coupling terms open gaps everywhere two branches of the folded parabola cross, *i.e.* in the center and on the boundaries of the first Brillouin zone. The gap near a crossing of two unperturbed branches labeled by p_1 and p_2 appears at a perturbation order

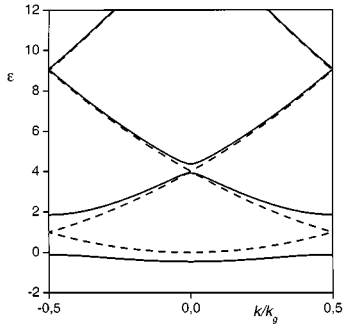

Fig. 2. Plots of the energies ε of the lowest Bloch states belonging to the first Brillouin zone *versus* the reduced quasimomentum $k/k_{\rm g}$. The energy unit is $\hbar\omega_{\rm rec}$ and we have plotted the energy diagram for two values of the potential strength parameter $q = V_0/4\hbar\omega_{\rm rec}$: solid line $q = 1$, dashed line, $q = 0$. The energy shift $V_0/2$ has been omitted.

$n = |p_1 - p_2|$ and, as long as q is not too large, the effective coupling between two levels can be calculated at the lowest nonvanishing order of perturbation theory [7,8,21]. When q is small ($q \lesssim 1$), the effective coupling decreases rapidly with the order n and this fact explains why the high-n gaps are too small to be visible. This is illustrated in Figure 2 where the energies $\varepsilon(k,p)$ are plotted as a function of k and p for $q = 0$ and 1. The common shift of all the energy levels due to the term $V_0/2$ does not appear as this term has been omitted in equation (3). The calculations necessary to produce the plots of Figure 2 are made in a truncated basis of free Bloch states. The size of the basis set necessary to get converged results can be evaluated using semiclassical arguments. This size is comparable to the number of discrete bound states in a well corresponding to one period of the potential V, which is given by $4\sqrt{q}/\pi$.

4 Continuity equations and diffraction amplitudes

We now write the general form of the solution in the three different regions of space and the continuity of the atomic wave on the boundaries. Continuity for all times ensures energy conservation. On a boundary, the wavefunction and its normal derivative must be continuous. If we assume for example the boundary to be the $z = 0$ plane, the continuity equations take the form:

$$\Psi(z=0^-) = \Psi(z=0^+) \quad \text{and} \quad \frac{\partial\Psi}{\partial z}(z=0^-) = \frac{\partial\Psi}{\partial z}(z=0^+). \quad (9)$$

These two continuity equations can be fulfilled together only if we consider a reflected wave. Here, we will neglect any atomic wave reflected by the boundaries. This is a good approximation because the potential V_0 is very weak with usual laser power densities. We have already assumed in Section 2 that V_0 is considerably smaller than the atom kinetic energy E and this is justified as long as the atoms are not ultra-cold. Moreover, the transitions between the vacuum and the grating in the planes $z = 0$ and $z = D$ occur on distances which are always larger than the laser wavelength and therefore considerably larger than the atomic wavelength; this circumstance further reduces the amplitude of the reflected wave. When neglecting the reflected wave, the two continuity equations are equivalent and we will use the continuity of the wavefunction.

In this part, we will use Dirac notations. In region 1, which is free space with $z \leq 0$, the incident atomic wave is assumed to be described by a plane wave

$$|\Psi_1\rangle = |k_{x1}\rangle\,|k_{z1}\rangle\,. \quad (10)$$

In region 2, inside the grating $0 \leq z \leq D$, the transmitted wave is described by a sum of products of Bloch states noted $|k,p_2\rangle$ (for the x motion) by plane waves describing the z motion:

$$|\Psi_2\rangle = \Sigma_{k,p_2} b_{p_2}(k)\,|k,p_2\rangle\,|k_{z2}(k,p_2)\rangle\,. \quad (11)$$

In region 3, the transmitted wave can be written as a sum of plane waves

$$|\Psi_3\rangle = \Sigma_{p_3} c_{p_3}\,|k_{x3}(p_3)\rangle\,|k_{z3}(p_3)\rangle\,. \quad (12)$$

In the plane $z = 0$, the continuity of the wavefunction proves that the non vanishing coefficients $b_{p_2}(k)$ are those for which k is the image of k_{x1} in the first Brillouin zone. This reduces the double sum over k and p_2 appearing in equation (11) to a single sum over p_2. To calculate the coefficients $b_{p_2}(k)$, we write $\langle z=0|\Psi_1\rangle = \langle z=0|\Psi_2\rangle$ and we introduce a sum rule using the Bloch state basis set, which is equivalent to write the equality of the x-Fourier transform of these two wavefunctions. We thus get:

$$b_{p_2}(k) = \langle k,p_2|k_{x1}\rangle\,. \quad (13)$$

In the same way, continuity in the plane $z = D$ proves that the final states have the following x component of their wavevector:

$$k_{x3}(p_3) = k_{x1} + p_3 k_{\rm g}. \quad (14)$$

With this choice, the index p_3 is the usual diffraction order. Continuity provides the amplitudes of the various diffraction orders:

$$c_{p_3} = \Sigma_{p_2}\,\langle k_{x3}(p_3)|k,p_2\rangle\,\langle k,p_2|k_{x1}\rangle \times \exp\left[\mathrm{i}\left(k_{z2}(k,p_2) - k_{z3}(p_3)\right)D\right]. \quad (15)$$

Energy conservation writes:

$$\frac{\hbar^2(k_{x1}^2+k_{z1}^2)}{2m} = \varepsilon(k,p_2) + \frac{\hbar^2 k_{z2}(k,p_2)^2}{2m} = \frac{\hbar^2(k_{x3}^2+k_{z3}^2)}{2m}\,. \quad (16)$$

As long as q and $k_{x1}/k_{\rm g}$ are not too large, the important contributions in equation (15) come from small values of p_2 and, in this range, the dependence of $k_{z2}(k,p_2)$ with p_2 is small. Nevertheless, when the wave reaches the

plane $z = D$, the dependence with p_2 of the accumulated phases creates the diffraction effect. If the propagation phases appearing in equation (15) were independent of p_2, a sum rule would obviously appear in this equation and only one plane wave would be transmitted in medium 3, corresponding to the zeroth order of diffraction. In this formalism, diffraction appears very easy to calculate and to understand. In particular, an interesting point is that, inside the grating, the wave is split in an infinite series of different waves labeled by the index p_2 and having different wavevectors. This generalizes the treatment introduced for neutrons and adapted to the atomic case [16]. We are now going to test the present approach in the Raman-Nath and Bragg regimes.

5 Raman-Nath diffraction regime

Following the discussion presented by Keller *et al.* [21], this problem involves three main parameters. Two of them have already been discussed: the potential strength V_0 and the recoil energy $\hbar\omega_{\rm rec}$. The last parameter is the interaction time $t_{\rm int}$ of the atom with the grating. For an incidence not too far from normal incidence, the velocity v_z is closely approximated by $v_z \approx \hbar k_1/m$ and the interaction time is given by $t_{\rm int} = D/v_z \approx mD/\hbar k_1$. With these three parameters, we can build two dimensionless parameters, namely q already introduced (Eq. (8)) and a reduced interaction time $\tau_{\rm int}$ given by:

$$\tau_{\rm int} = \omega_{\rm rec} t_{\rm int}. \tag{17}$$

With these notations and using the fact that $E \gg V_0$, the phase appearing in the exponential in equation (15) can be given a very simple form:

$$\left(k_{z2}(k,p_2) - k_{z3}(p_3)\right) D \simeq -\frac{1}{\hbar}\left(\varepsilon_0(k,p_3) - \varepsilon(k,p_2)\right) t_{\rm int}. \tag{18}$$

The Raman-Nath approximation consists in neglecting the dynamics of the atom inside the region where the potential $V(x,z)$ is nonvanishing. This is a good approximation when the interaction time is short enough. A classical treatment of the dynamics should give a good estimate of the validity regime. Developing $V(x,z)$ up to second order in x near one of its minima, the oscillation angular frequency is given by:

$$\omega_{\rm osc} = 4\omega_{\rm rec}\sqrt{q}. \tag{19}$$

When the oscillation phase given by $\omega_{\rm osc} t_{\rm int}$ is close to 1 radian, we have reached the upper limit where the dynamics inside the potential V is expected to be negligible. This condition writes:

$$\tau_{\rm int} < \frac{1}{4\sqrt{q}}\,. \tag{20}$$

A similar condition appears in the paper by Keller *et al.* ($\tau_{\rm int} < 1/(2\sqrt{2q})$). In the Raman-Nath approximation, for an incident beam at normal incidence, the diffraction probability in the nth order is a very classical result [14,24] given by:

$$P_n = \left|J_n(\gamma)\right|^2 \tag{21}$$

where $\gamma = 2q\tau_{\rm int}$ is the amplitude of the phase modulation. With the present formalism, the demonstration of this analytic formula is not at all straightforward. This is not surprising as the Raman-Nath formula is exact only in the limit $q \to \infty$ and $\tau_{\rm int} \to 0$, while keeping a finite value to the phase $\gamma = 2q\tau_{\rm int}$. The description of the Bloch states in the $q \to \infty$ limit requires a nonperturbative approach. Moreover, the validity range of the Raman-Nath formula is narrow as shown by Berry [24], who has calculated the next terms of the $1/q$ expansion. The compact character of equation (21) makes it very attractive and somewhat obscures its narrow validity range (see also the discussion by Henkel [25]). Using our formalism, it is easy to calculate numerically the diffraction intensity for the first diffraction orders. We have sampled the range 1–1000 for the potential strength parameter q and the range 0–16 for the phase γ. The calculated intensities of the zeroth and first order diffraction peaks are plotted in Figure 3. For the limited interaction times considered in these calculations, the basis set necessary to get converged results remains rather small: for instance, when $q = 1000$, our calculations are converged with a basis size equal to 41 (as verified by increasing the basis size to 61).

6 The Bragg regime

Diffraction in the Bragg regime can provide ideal tools such as mirrors and beam splitters for atomic interferometers [7,8]: the exit beam is split in only two beams and their relative intensities can be tuned by varying the potential strength V_0 or the interaction time $t_{\rm int}$. We consider here only the case of first order diffraction *i.e.* when $k_{x1} \simeq k_{\rm g}/2$ (higher order diffraction is very similar as shown by Giltner *et al.* [7,8]). We note $k_{x1} = (1-\kappa)k_{\rm g}/2$ and we assume that κ is positive so that k_{x1} belongs to the first Brillouin zone. Then, the exact calculation of Bloch states reduces to a two level problem completely similar to the Rabi oscillation. These two levels noted $|0\rangle$ and $|-1\rangle$ are the levels:

$$|0\rangle = |k_{x1}, p = 0\rangle \text{ and } |-1\rangle = |k_{x1}, p = -1\rangle \tag{22}$$

where we have used the notations introduced by equation (6). These two unperturbed levels represent the plane waves with the x-component of the wavevector equal to k_{x1} and $k_{x1} - k_{\rm g}$, corresponding respectively to the diffraction orders 0 and -1. When $V_0 = 0$, the energy of these unperturbed levels are, after shifting the energy zero to a convenient value, $\varepsilon_0 = -\Delta/2$ and $\varepsilon_{-1} = +\Delta/2$, where $\Delta = 4\hbar\omega_{\rm rec}\kappa$. In the presence of a potential, the coupling terms between these two levels are just equal to $V_0/4$. The Bloch eigenstates result from the diagonalization of the 2×2 Hamiltonian:

$$H = \begin{bmatrix} -\Delta/2 & V_0/4 \\ V_0/4 & \Delta/2 \end{bmatrix} = \hbar\omega_{\rm rec} \begin{bmatrix} -2\kappa & q \\ q & 2\kappa \end{bmatrix} \tag{23}$$

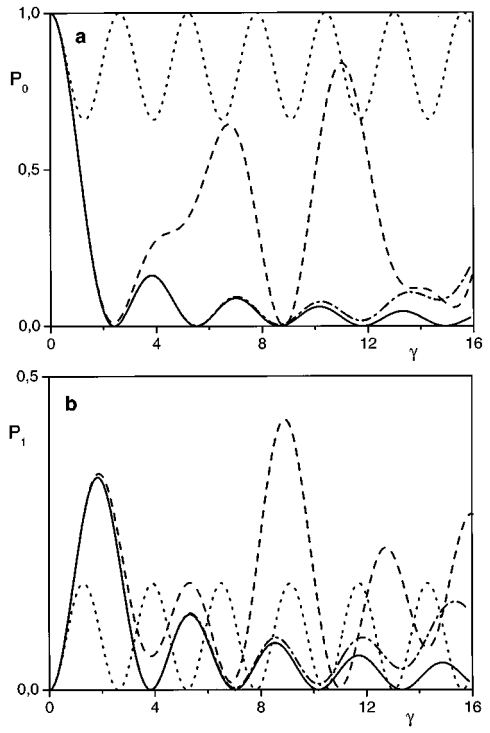

Fig. 3. Plot of the diffraction intensity in the zero order P_0 (part a) and first order P_1 (part b) for normal incidence and for various q values as a function of the product $\gamma = 2q\tau_{\rm int}$: solid line $q = 1000$, dot-dashed line $q = 100$, dashed line $q = 10$ and dotted line $q = 1$. The validity of the Raman-Nath formula (Eq. (21)) for the two diffraction orders tested here is excellent when $q = 1000$ up to our largest γ value. The validity range shrinks rapidly when q decreases: the deviation from the Raman-Nath formula (21) appears near $\gamma = 5$ with $q = 100$, near $\gamma = 1.5$ when $q = 10$ and near $\gamma = 0.5$ for $q = 1$, in excellent agreement with the validity range $\gamma < \sqrt{q}/2$ deduced from condition (20). Finally, the behaviour for $q = 1$, which reminds the Rabi oscillation observed in the Bragg regime, can be explained: the problem involves almost only the three lowest Bloch states describing the plane waves with $k_x = 0, \pm k_{\rm g}$ and the symmetry associated to normal incidence makes that the $k_x = 0$ state is coupled only to the symmetric combination of the other states. This symmetry reduces the problem to a two-level problem.

with the following energies:

$\varepsilon_\pm = \pm\hbar\Omega/2$ with

$$\hbar\Omega/2 = \sqrt{\left(\frac{\Delta}{2}\right)^2 + \left(\frac{V_0}{4}\right)^2} = \hbar\omega_{\rm rec}\sqrt{q^2 + 4\kappa^2}. \quad (24)$$

These energies plotted as a function of k_{x1} exhibit a characteristic avoided crossing, as illustrated by Figure 4. The eigenstates are given by:

$$|+\rangle = \cos\theta\,|-1\rangle + \sin\theta\,|0\rangle$$
$$\text{and } |-\rangle = -\sin\theta\,|-1\rangle + \cos\theta\,|0\rangle\,. \quad (25)$$

The mixing angle θ such that $0 \le \theta < \pi/2$ is defined by

$$\tan 2\theta = V_0/(2\Delta) = q/(2\kappa). \quad (26)$$

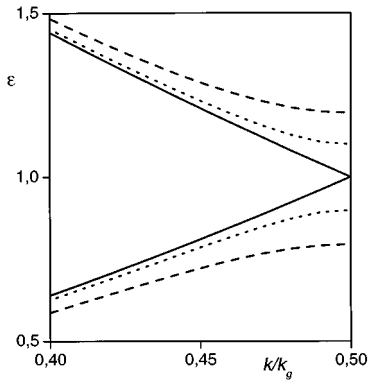

Fig. 4. Detail of the energy diagram of Figure 2 near the border of the first Brillouin zone around the energy $\varepsilon = \hbar\omega_{\rm rec}$. The three curves correspond to the case $q = 0$ (full line), $q = 0.1$ (dotted line), $q = 0.2$ (dashed line). The avoided crossing which plays the central role in first order Bragg scattering is clearly visible.

The initial state can be expressed as a function of the Bloch states:

$$|k_{x1}\rangle = |0\rangle = \sin\theta\,|+\rangle + \cos\theta\,|-\rangle\,. \quad (27)$$

Taking into account the propagation through the grating, we get the wavefunction in the exit plane $z = D$:

$$\langle z = D|\Psi_2\rangle = \sin\theta\exp(\mathrm{i}k_z^+ D)\,|+\rangle + \cos\theta\exp(\mathrm{i}k_z^- D)\,|-\rangle \quad (28)$$

where $k_z^\pm$ are the z-component of the wavevector associated to these two internal states. Their values are deduced from energy conservation (Eq. (16)) and their difference is given by (see also Eq. (18)):

$$k_z^+ - k_z^- \approx -\frac{\varepsilon_+ - \varepsilon_-}{\hbar v_z}\,. \quad (29)$$

When expressed in the free basis set ($|0\rangle$ and $|-1\rangle$), this wavefunction gives the amplitudes of diffraction in the zero and first orders. The probability P_1 of diffraction in the first order is given by:

$$P_1 = \frac{V_0^2}{V_0^2 + 4\Delta^2}\sin^2\left(\frac{\Omega t_{\rm int}}{2}\right) = \frac{q^2}{q^2 + 4\kappa^2}\sin^2\left(\tau_{\rm int}\sqrt{q^2 + 4\kappa^2}\right) \quad (30)$$

which is just the Rabi oscillation formula applied to Bragg diffraction. This formula has been written before many times [7,8,16]. When k_{x1} is just outside the first Brillouin zone, κ is negative, but the calculation remains the same, except that the initial state is now the state $|-1\rangle$. This does not modify the diffraction probability still given by equation (30).

This formula gives useful information on the selectivity with k_{x1} (or with κ) of the Bragg diffraction process.

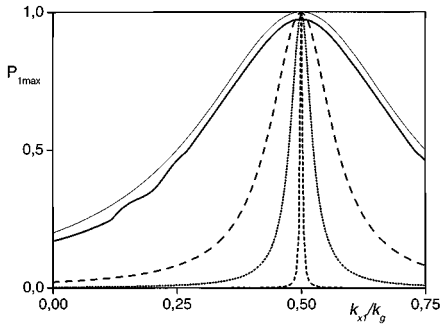

Fig. 5. Plot of the maximum intensity $P_{1\,\max}$ that can be reached in first diffraction order as a function of the reduced incident momentum $k_{x1}/k_{\rm g}$. For $k_{x1} = k_{\rm g}/2$, the Bragg condition is fulfilled. Solid lines $q = 1$: the thin line represents the result of the two-level calculation, while the full thicker line represents the result of the complete calculation. For smaller values of q, the difference between these two calculations is too small to be visible at the scale of the figure. Long-dashed line: $q = 0.3$, dotted line: $q = 0.1$, dashed line: $q = 0.01$.

Using the phase $\gamma = 2q\tau_{\rm int}$ defined previously and a dimensionless parameter $Y = 2\Delta/V_0 = 2\kappa/q$, we get:

$$P_1 = \frac{1}{1+Y^2}\sin^2\left(\frac{\gamma\sqrt{1+Y^2}}{2}\right). \qquad (31)$$

The diffraction efficiency reaches a maximum value equal to $1/(1+Y^2)$ for the optimum value of the phase γ (*i.e.* of the interaction time $t_{\rm int}$). We plot in Figure 5 this maximum value of the probability P_1 as a function of k_{x_1} for different values of the parameter q. We compare in this figure the prediction of equation (31) with the results of a numerical calculation, in which the two-level hypothesis is relaxed (P_1 is calculated as a function of $t_{\rm int}$ by the computer program which then extracts its maximum value). As expected from the inspection of Figure 4, when q is small, the avoided crossing in the Bloch state energy diagram is very narrow, the two level hypothesis is an excellent approximation and the diffraction process is very sensitive to the value of k_{x_1}. On the contrary, when one works with a substantial value of the potential strength parameter q ($q \approx 1$), the selectivity with the value of k_{x_1} is rather poor and at the same time, the two level calculation deviates from the numerical result.

The parameter Y measures the distance to the Bragg condition in a real experiment. For instance, if the beam has a negligible angular dispersion and $v_{\rm Bragg}$ represents the velocity corresponding to the Bragg condition for the incidence angle, then Y is proportional to the velocity difference $\Delta v = (v - v_{\rm Bragg})$, (exactly, $Y = 2\Delta v/(qv_{\rm Bragg})$). In the same way, if the velocity dispersion is negligible and $i_{\rm Bragg}$ is the Bragg incidence angle for the mean velocity, Y is proportional to the difference in incidence angle $\Delta i = (i - i_{\rm Bragg})$, (exactly, $Y = 2\Delta i/(qi_{\rm Bragg})$). In both cases, the diffraction probability P_1 is a resonant function whose width is proportional to q.

7 Discussion

An important question concerns the practical interest of our calculation: we have introduced somewhat artificially discontinuities in the plane $z = 0$ and $z = D$, which do not exist in a real experiment. An adiabatic argument suggests that in the absence of any discontinuity, the initial free state transforms adiabatically in a single Bloch state which transforms back to the same free state when the atom emerges out of the laser standing wave. Nevertheless, non adiabatic transitions can occur even in a potential having a smooth and bell-shaped envelope $V_0(z)$. We will assume that the potential $V_0(z)$ is fully negligible outside a region defined by $z_i < z < z_f$. We discuss here the case of first order Bragg scattering with $q \ll 1$, so that we can consider only two levels as in the previous section, but we think that the argument is general. In the basis set defined above (Eq. (22)), we have now to integrate the Schrödinger equation as a function of z (see Appendix A):

$$\mathrm{i}\hbar v_z \frac{\partial\psi(x,z)}{\partial z} = H\psi(x,z) \qquad (32)$$

where the Hamiltonian H is given by equation (23) in which V_0 is now a function of z. Let us first consider that the incidence angle is such that the Bragg condition is exactly fulfilled, $k_{x1} = k_{\rm g}/2$. Then, the two levels are exactly degenerate ($\Delta = 0$) when the potential vanishes. In the presence of such a degeneracy, the adiabatic argument is obviously not valid. This case corresponds to the resonance Rabi oscillation which is exactly solvable whatever the function $V_0(z)$. Assuming the same initial conditions as above, we get the probability P_1 of first order diffraction:

$$P_1 = \sin^2(\varphi) \quad \text{with} \quad \varphi = \int_{z_i}^{z_f} \frac{V_0(z)}{4\hbar v_z}\mathrm{d}z. \qquad (33)$$

If the incidence angle is not exactly equal to the Bragg angle, Δ is nonzero but small ($\Delta \ll \hbar\omega_{\rm rec}$), the adiabatic argument is valid in the far wings of $V(z)$, where $V(z) \ll \Delta$, but, in the region where $V(z) \approx \Delta$, the eigenstates of the 2×2 Hamiltonian (Eq. (23)) rotate rapidly as a function of z. The behaviour will be nonadiabatic in the regions where the following condition holds:

$$\mathrm{d}\theta/\mathrm{d}t \gtrsim \Omega/2 \qquad (34)$$

where θ and Ω are defined by equations (26, 24) respectively. With the present notations, a nonadiabatic behaviour occurs when:

$$4\hbar v_z \left|\Delta\frac{\mathrm{d}V_0(z)}{\mathrm{d}z}\right| \gtrsim \left(4\Delta^2 + V_0^2(z)\right)^{3/2}. \qquad (35)$$

Then it is a good approximation to assume that the transitions from free states ($V_0(z) \ll \Delta$) to Bloch states ($V_0(z) \gg \Delta$) and backwards are sudden. In this case, although the potential envelope $V_0(z)$ is smooth, the atomic dynamics can be described in a discontinuous manner. This discontinuous dynamics is precisely what we have

introduced in our model calculation in the plane $z = 0$ and $z = D$. With a smooth potential, the sudden changes occur probably near the z values for which $V_0(z) = \Delta$, but their exact location depends of the shape of $V_0(z)$ and of the velocity v_z. In the entrance pathway, the initial state is projected on the Bloch states which are projected backwards on the free states in the exit pathway. These two non adiabatic events occur in the region defined by equation (35). The propagation of the two Bloch states involves a phase difference which plays the role of the phase of the sine in equation (30). This behaviour can be illustrated in an exactly solvable case. Because laser beams are often well described by Gaussian functions, it would be interesting to consider a potential $V_0(z) = V_G \exp(-2z^2/w_G^2)$ proportional to light intensity (where w_G is the beam waist radius). Unfortunately, in this case, we do not know any analytic solution. We will therefore consider a hyperbolic secant case for which an analytic solution exists [27,28]:

$$V_0(z) = V_{SH}/\cosh(z/w_{SH}). \tag{36}$$

One should keep in mind that the hyperbolic secant pulse has longer wings than the Gaussian pulse. The transition probability in this case is given by:

$$P_1 = \frac{\sin^2(\pi V_{SH} w_{SH}/4\hbar v_z)}{\cosh^2(\pi \Delta w_{SH}/2\hbar v_z)}\,. \tag{37}$$

In the case $\Delta = 0$, as expected, this is just the general result given by equation (33). When $\Delta w_{SH}/\hbar v_z$ becomes larger than 1, the transition probability decreases rapidly as expected from the adiabaticity argument. Except when $|z|$ is small, $|z| \lesssim w_{SH}$, the derivative of $V_0(z)$ is closely approximated by $\pm V_0(z)/w_{SH}$. Then with this approximation, the condition (35) is most easily fulfilled near the point where $V_0(z) = \Delta/\sqrt{2}$ and at this point, the nonadiabaticity condition is given by:

$$|\Delta| \leq 2\hbar v_z/(3\sqrt{3} w_{SH}). \tag{38}$$

When Δ reaches this limit, the diffraction efficiency is still as large as 0.71. For larger Δ values, the diffraction efficiency becomes rapidly very small because the behaviour is adiabatic everywhere. Equation (37) can be used to study the selectivity of Bragg scattering in a more realistic case than previously. Assuming that the phase of the sine is optimized (this phase must be equal to $\pi/4$ for a beam-splitter and to $\pi/2$ for a mirror), the angular or velocity selectivity comes only from the denominator. This result is somewhat peculiar to the hyperbolic secant pulse for which the power broadening appearing in the Rabi formula has no equivalent.

8 Conclusion

The Bloch state description appears to be a very good tool to understand atomic diffraction in a unified manner. The Bloch states can be viewed as an extension of the dressed atom picture [22] from the energy spectrum to the momentum domain. In the dressed atom picture, the spontaneous emission process plays an important dynamical role: the atom can jump from one multiplicity to the next one through spontaneous emission. If the atomic dressing involves momentum, the problem becomes rapidly very complex as the momentum is a vector in 3D. Because the momentum transfer due to spontaneous emission can take any direction, the evolution in the momentum space is not easily visualized. The large simplification here comes from the 1D character of the laser waves and from the absence of spontaneous emission, both being necessary to keep an effective 1D character to the momentum problem.

We have shown that simple numerical calculations can be used to calculate atomic diffraction for almost any case as long as the parameter q measuring the strength of the potential is not very large compared to 1. We can thus describe all the different regimes studied up to now: Raman-Nath, Bragg and channeling (this last case has not been studied here in order to focus on the simplest ones). However, the calculation is very simple only if we assume a rectangular intensity profile for the laser standing wave. This simple calculation provides physical insight, but, obviously, this is not always a good approximation. Finally, we have discussed the validity of this approximation in the case of Bragg diffraction, as this regime appears to be of greatest practical interest.

This work can be extended to study several other cases:

- the Bragg diffraction regime has been studied as involving only two Bloch states and this is just a rewording of previous works (see the review by Bordé [16] and references therein). The real problem involves an infinity of states, among which one other state is also strongly coupled and is not very far away. This nonresonant coupling should play a role comparable to the one of the counter rotating wave in magnetic resonance, creating the Bloch-Siegert shift. We think that this is an important question as some phaseshifts could be due to this effect;
- the present treatment can be generalized to other diffraction processes, for instance involving Raman transfer among hyperfine levels [29–32];
- the present formalism can probably be extended to represent atomic diffraction by material gratings, including the effects of the atom-grating van der Waals interaction [26].

We are very much indebted to G. Bastard, J. Dalibard, A. Aspect for very helpful discussions, to C. Keller for providing us a preprint of reference [21], to N. Vitanov for an illuminating course on coherent atomic excitation by laser pulses and to one of our referees for pointing out to us the work of Wagner [23]. Région Midi-Pyrénées is gratefully acknowledged for financial support given to our laboratory.

Appendix A

Starting from the Schrödinger equation (2):

$$-\frac{\hbar^2}{2m}\left(\frac{\partial^2 \Psi}{\partial x^2} + \frac{\partial^2 \Psi}{\partial z^2}\right) + V(x,z)\Psi = \frac{\hbar^2 k_1^2}{2m}\Psi \tag{39}$$

this equation can be simplified if one assumes that the total energy $E = \hbar^2 k_1^2/2m$ is large ($E \gg V(x,z)$) and that the wavevector is almost parallel to the z-axis. One then searches an approximate solution Ψ of the form:

$$\Psi = \exp(\mathrm{i}k_1 z)\psi(x,z) \tag{40}$$

where the z-dependence of $\psi(x,z)$ is assumed to be small so that one can neglect the second derivative with respect to z. This gives:

$$\frac{\mathrm{i}\hbar^2 k_1}{m}\frac{\partial\psi}{\partial z} = -\frac{\hbar^2}{2m}\frac{\partial^2\psi}{\partial x^2} + V(x,z)\psi. \tag{41}$$

One recognizes the velocity $v_z = \hbar k_1/m$ and this equation takes the final form:

$$\mathrm{i}\hbar v_z \frac{\partial\psi}{\partial z} = H_x\psi. \tag{42}$$

Here $H_x = -\frac{\hbar^2}{2m}\frac{\partial^2}{\partial x^2} + V(x,z)$ is the Hamiltonian describing the dynamics in the **x**-direction. If one puts $t = z/v_z$, one gets the usual time-dependent Schrödinger equation in the quasi-classical limit, where velocity v_z is assumed to be constant.

Appendix B

In his book [24], Berry has studied diffraction of light by acoustic waves: the medium of thickness D is described by its refraction index $\mu_0 + \mu_1\cos(b\eta)$ where the second term is the small modulation due to the acoustic wave (the slow time dependence being neglected). The wave equation for light (Eq. (4.1.1) of [24]) is:

$$\frac{\partial^2\phi}{\partial\eta^2} + \frac{\partial^2\phi}{\partial\xi^2} + k^2\mu_0^2\left(1 + \frac{2\mu_1\cos(b\eta)}{\mu_0}\right)\phi = 0. \tag{43}$$

This equation is strictly equivalent to our equation (3) if one uses the following correspondence: $\eta \to x$, $\xi \to z$, $\phi \to \Psi$, $k\mu_0 \to k_1$, $(2\mu_1/\mu_0) \to (-V_0/2E)$, $b \to k_\mathrm{g}$. Berry introduces two dimensionless parameters defined by $\rho = b^2/(\mu_0\mu_1 k^2)$ and $x = k\mu_1 D$ (not to be taken for our x coordinate). The translation in our notations is straightforward: ρ becomes $-1/q$ and x becomes $-\gamma = -2q\tau_\mathrm{int}$.

The intensities of the first diffraction orders as a function of $x = -\gamma$ obtained by numerical calculations with an analogue computer are plotted by Berry [24] (Figs. 11–13, pp. 110–112) for various values of the parameter ρ. We have recalculated these curves with our technique and the curves we obtain are extremely similar (as illustrated by Fig. 3), if we accept to consider that the ρ values given by Berry are too large by a factor 4. We have no explanation for this discrepancy.

References

1. P.E. Moskowitz, P.L. Gould, S.R. Atlas, D.E. Pritchard, Phys. Rev. Lett. **51**, 370 (1983).
2. P.L. Gould, D.E. Pritchard, J. Opt. Soc. Am. B **2**, 1799 (1985).
3. P.L. Gould, G.A. Ruff, D.E. Pritchard, Phys. Rev. Lett. **56**, 827 (1986).
4. P.J. Martin, P.L. Gould, B.G. Oldaker, A.H. Miklich, D.E. Pritchard, Phys. Rev. A **36**, 2495 (1991).
5. P.L. Gould, P.J. Martin, G.A. Ruff, R.E. Stoner, J.L. Picqué, D.E. Pritchard, Phys. Rev. A **43**, 585 (1991).
6. P.J. Martin, B.G. Oldaker, A.H. Miklich, D.E. Pritchard, Phys. Rev. Lett. **60**, 515 (1988).
7. D.M. Giltner, R.W. McGowan, Siu Au Lee, Phys. Rev. A **52**, 3966 (1995).
8. D.M. Giltner, R.W. McGowan, Siu Au Lee, Phys. Rev. Lett. **75**, 2638 (1995).
9. E.M. Rasel, M.K. Oberthaler, H. Batelaan, J. Schmiedmayer, A. Zeilinger, Phys. Rev. Lett. **75**, 2633 (1995).
10. M.K. Oberthaler, R. Abfalterer, S. Bernet, J. Schmiedmayer, A. Zeilinger, Phys. Rev. Lett. **77**, 4980 (1996).
11. S. Bernet, M.K. Oberthaler, R. Abfalterer, J. Schmiedmayer, A. Zeilinger, Phys. Rev. Lett. **77**, 5160 (1996).
12. R. Abfalterer, C.M. Keller, S. Bernet, M.K. Oberthaler, J. Schmiedmayer, A. Zeilinger, Phys. Rev. A **56**, R4365 (1997).
13. C.M. Keller, M.K. Oberthaler, R. Abfalterer, S. Bernet, J. Schmiedmayer, A. Zeilinger, Phys. Rev. Lett. **79**, 3327 (1997).
14. A.F. Bernhardt, B.W. Shore, Phys. Rev. A **23**, 1290 (1981).
15. C. Tanguy, S. Reynaud, C. Cohen-Tannoudji, J. Phys. B: At. Mol. Phys. **17**, 4623 (1984).
16. C.J. Bordé, *Atom interferometry*, edited by P.R. Berman (Academic Press, 1997), p 257.
17. Y. Castin, J. Dalibard, Europhys. Lett. **14**, 761 (1991).
18. M. Ben Dahan, E. Peik, J. Reichel, Y. Castin, C. Salomon, Phys. Rev. Lett. **76**, 4508 (1996).
19. S.R. Wilkinson, C.F. Bharucha, K.W. Madison, Quian Niu, M.G. Raizen, Phys. Rev. Lett. **76**, 4512 (1996).
20. M. Horne, I. Jex, A. Zeilinger, Phys. Rev. A **59**, 2190 (1999).
21. C. Keller, J. Schmiedmayer, A. Zeilinger, T. Nonn, S. Dürr, G. Rempe, Appl. Phys. B **69**, 303 (1999).
22. C. Cohen-Tannoudji, J. Dupont-Roc, G. Grynberg, *Atom-photon interactions* (Wiley Science Paperback, 1998).
23. E.H. Wagner, Z. Phys. **141**, 604 and 622 (1955).
24. M.V. Berry, *The diffraction of light by ultrasound* (Academic Press, London, 1966).
25. C. Henkel, J.-Y. Courtois, A. Aspect, J. Phys. II France **4**, 1955 (1994).
26. R.E. Grisenti, W. Schöllkopf, J.P. Toennies, G.C. Hegerfeldt, T. Köhler, Phys. Rev. Lett. **83**, 1755 (1999).
27. N. Rosen, C. Zener, Phys. Rev. **40**, 502 (1932).
28. N.V. Vitanov, J. Phys. B: At. Mol. Opt. Phys. **31**, 709 (1998).
29. U. Gaubatz, P. Rudecker, M. Becker, S. Schiemann, M. Külz, K. Bergmann, Chem. Phys. Lett. **149**, 463 (1988).
30. P. Marte, P. Zoller, J.L. Hall, Phys. Rev. A **44**, R4118 (1991).
31. M. Kasevich, S. Chu, Phys. Rev. Lett. **67**, 181 (1991).
32. M. Weitz, B.C. Young, S. Chu, Phys. Rev. Lett. **73**, 2563 (1994).